Satellite gravity anomaly and vertical gradient fields corrected for topographic effect in the South Central Andes region

I.G.S.V.

Alvarez Pontoriero, Orlando1; Gimenez, Mario Ernesto1; Braitenberg, Carla2; Spagnotto, Silvana1

1 Instituto Geofísico-Sismológico Volponi, Universidad Nacional de San Juan, Argentina
2 Dipartimento di Geoscienze, Università di Trieste, Via Weiss 1, 34100 Trieste, Italy.

Abstract

Mass inhomogeneities affect the Earth gravity field. The satellite missions CHAMP, GRACE and now GOCE have introduced an extraordinary improvement in the global mapping of the gravity field, either through the orbit monitoring, or through acceleration and gradient measurements at satellite height. Global models based on observations of satellite data plus terrestrial data are available in spherical harmonic expansion with maximum degree and order of 2159 (Pavlis et al., 2008); global models based on the observations of satellite GOCE are available up to degree and order N=250. This allows us to study the crust and lithosphere at regional scale. Gradients of the gravity field highlights main geological features such as volcanic deposits, sutures, lineaments (Braitenberg et al. 2011). The gravity gradient tensor (Marussi tensor) is composed by five independent elements and is obtained as the second derivatives of the disturbing potential (e.g. Hoffmann-Wellenhof and Moritz, 2005), while gravity anomaly is obtained as the first spatial derivative. For geological mapping the vertical derivative of the gravity anomaly (Tzz component) is ideal, as it highlights the center of the anomalous mass (Braitenberg et al., 2011).

The vertical gravity gradient and the gravity field for south Central Andes are calculated (Janak and Sprlak, 2006) using the global model EGM-2008. The calculation height is 7000m to ensure that all values are above the topography and is made in a spherical coordinate system. The values are calculated on a regular grid of 0.05° grid cell size, with a maximum degree and order equal to 2160 of the harmonic expansion. We control the quality of the terrestrial data entering the EGM08 by a comparison analysis with the observations from GOCE. The topographic effect is removed from the fields to eliminate the correlation with the topography, which is modeled with Smith and Sandwell (2003). Topographic mass elements are approximated with prismatic mass elements in spherical coordinates (Forsberg, 1983). Thus the topography corrected vertical gravity gradient and the topography corrected gravity anomaly are obtained. Comparison with geologic maps and known tectonic structures clearly highlights the contact between Pacific oceanic crust and Andean Mountains, thrust and fold belt, and Pampean Ranges. The Bermejo-Desaguadero lineament, the Tucuman lineament, and a new lineament that may be the continuation of the ridge between latitudes 26°S and 28°S, can be also clearly depicted.

The gravity gradient correlates well with the geologic map and to known lineaments, adding the advantage of regional area coverage obtained from satellite data. Therefore this is an advanced and powerful tool that can be used to obtain new information for understanding the tectonics of the region.

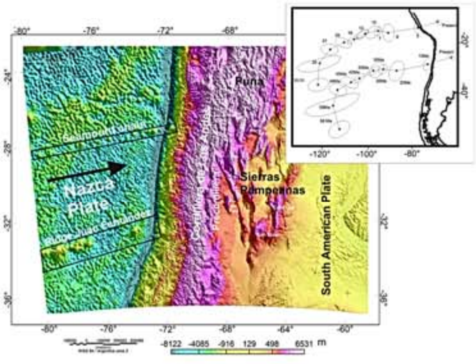

Figure 1: South Central Andes Region. Nazca Plate. South American Plate. Andean Ranges and geographical units. Convergence direction and ages

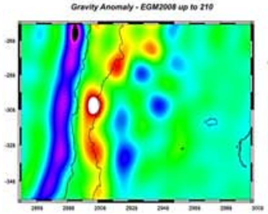

Figure 2: South Central Andes Region Gravity Anomaly up to 210 calculated (Janak and Sprlak, 2006) with EGM2008 (Plavlis, et. al, 2008).

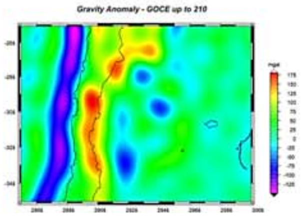

Figure 3: South Central Andes Region Gravity Anomaly up to 210 calculated (Janak and Sprlak, 2006) with GOCE data (Migliaccio et al., 2010).

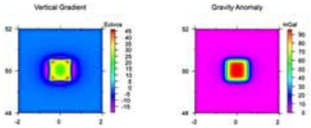

Figure 4: Vertical gravity gradient Vs Gravity anomaly generated by a topographic prism (Uieda et. al., 2010).

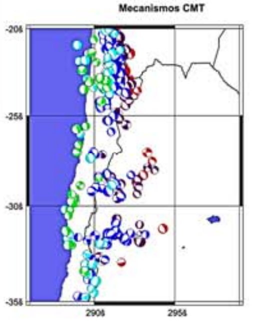

Figure 5: Focal mechanisms from CMT catalog with 70-170 km depth. Green 70/90km, Skyblue 90/110km, Blue 110/130km, Violet 130/150km, Red 150/170km.

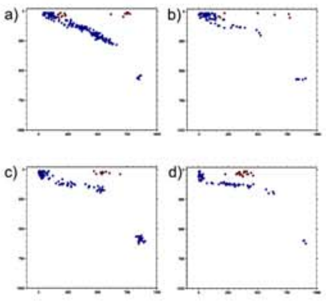

Figure 6: Crossection at 24.5°S(a), 26.5°S(b), 28.5°S(c) and 31.5°S(d); azimuth 82.2° ; +/- 150 km wide; 0-650 km depth.

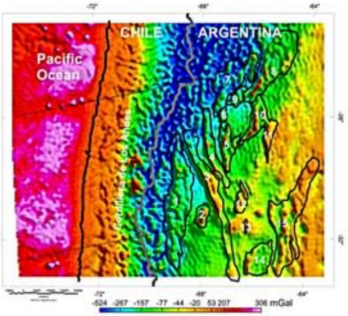

Figure 7: South Central Andes Region Gravity Anomaly corrected by topographic effect (Forsberg, 1984).

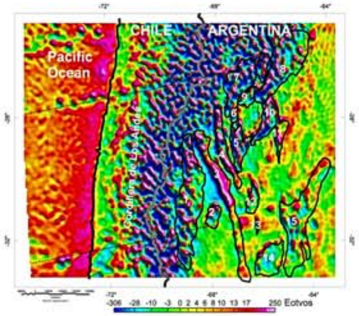

Figure 8: South Central Andes RegionVertical Gravity Gradient Tensor corrected by topographic effect (Forsberg, 1984)

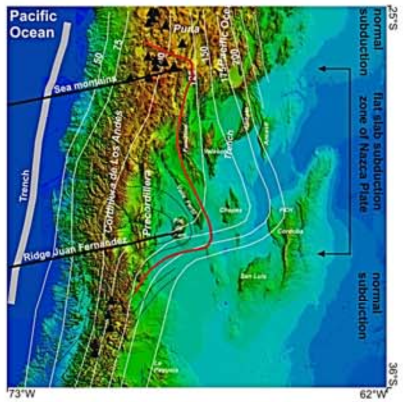

Figure 11: The solid white lines are contours of the top of the subducted Nazca plate from Cahill and Isacks (1992). Dashed black line contours mark slab depths from Anderson et al. (2007). Triangles are active volcanoes from Stern (2004). The solid red line is the proposed contour for the subducted Nazca plate.

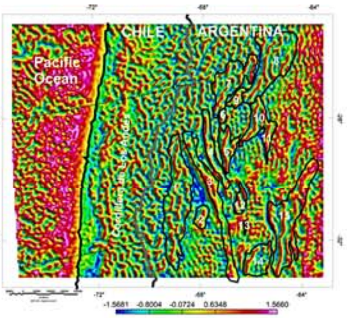

Figure 9: South Central Andes Region Tilt of the Gravity Anomaly.

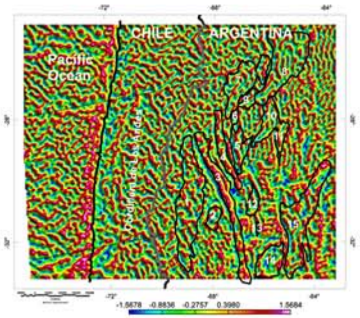

Figure 10: South Central Andes Region Tilt of the Vertical Gravity Gradient Tensor.

References: 1-Precordillera, 2-Pie de Palo, 3-Sistema de Sierras de Mas-Valle Fértil-Guayaguas-Catantal-Las Quijadas, 4) Sistema de Famatina, 5-Velasco, 6-Zapata y Vinquis, 7-Fiambalá, 8-Aconquija, 9-Capillitas, 10-Ambato, 11-Ancasti, 12-Chepes, 13-Ulapes, 14-San Luis y 15-Córdoba.

Summary and Concluding Remarks

Through a suitable processing of satellite gravimetric data, free air anomaly, gravity gradient tensor and tilt maps were generated and interpreted. In addition seismic focal mechanisms were analised. From these interpretations arise that the origin of Tucumán lineamient, located in the boundary region between the Pampean Sierras and the Puna, could be strongly related with the subduction of the seamounts chain on the Nazca plate. This phenomenon justifies the presence of major mineral manifestations of hydrothermal origin associated with Neogene volcanism over the Tucuman lineament trace (García, 1970a, Angelelli, 1984, Bassi, 1987, Rossello, 2000, among others), grouped in the informally called Farallón Negro Mining District (Bajo la Alumbrera, Capillitas, Agua Rica, Farallón Negro-Alto de la Blenda, among others).

It was also inferred that the flattened subduction of the Nazca plate should be controlled by the Juan Fernández Ridge at the southern region and by the subduction of the seamounts chain on its northern edge. Based on this, the geometry that best describes the roof of the subducted Nazca plate should be a combination between the two proposals (Figura 11): Cahill and Isacks (1992) and Anderson et al. (2007). Where in the Southern region would follow the proposal of these latter investigators, but in the northern region fits better with the proposal of Cahill and Isacks (1992) and would be associated with the changes in curvature of the subducted slab near 27°S to 28°S, from convex upward to concave upward, just downdip from the Nazca-South America plate boundary interface proposed by this authors. According to the proposed, the central Chile flat slab segment shows similar features with Peru flat slab segment that primarily identified by Barazangi and Isacks (1976). The southern portion of this flat slab has been atribuited to the subduction of the Nazca Ridge, but its northern portion remained unexplained until Gutscher et al. (1999a), who atribuited it to the completely subducted Inca Plateau. Later, Gustcher (2000) proposed that earthquake hypocenter data image two morphologic highs in the subductiong Nazca Plate which correlate with the positions of subducted oceanic plateaus.

Thus, evidence lead us to suppose that the central Chile flat slab should be contoled by the subduction of oceanic highs both to the north and to the south, as with the Peru flat slab.